

Dec 21, 2011

SEARCHING FOR HIGGS : FROM LEP TOWARDS LHC¹

W.-D. SCHLATTER¹ AND P. M. ZERWAS²

¹ Physics Department, CERN, CH-1211 Geneva, Switzerland

² Theory Group, DESY, D-22603 Hamburg, Germany

Abstract

After a brief introduction to the theoretical basis of the Higgs mechanism for generating the masses of elementary particles, the experimental searches for Higgs particles will be summarized, from bounds at LEP to inferences for LHC. The report will focus on the Standard Model, though some central results on extended Higgs systems, as conjectured for example in supersymmetric theories, will also be recapitulated. Alternative scenarios based on spontaneous symmetry breaking by novel strong interactions are adumbrated at the theoretical level.

1 Basics

1.1 General introduction

The fundamental laws of nature are formulated, at microscopic distances, in the Standard Model [SM] of particle physics [1–4]. The model consists of three elements:

- Leptons and quarks are the basic constituents of matter;
- The interactions are mediated by gauge fields;
- The masses are generated by the Higgs mechanism.

¹Report invited to the special volume “*CERN’s Accelerators, Experiments and International Integration 1959 – 2009*” of Eur. Phys. J. H, edited by H. Schopper (CERN, Geneva).

Experimental efforts have been devoted over nearly half a century to confront the theory with the structure of the real world.

The particles of the matter sector, fermionic leptons and quarks, arrange themselves in multiplets associated with underlying symmetry principles. Left-handed electrons and neutrinos, for example, are paired in doublets, originating from isospin symmetry, the corresponding right-handed particles however remain unpaired in singlets. The particles carry electric charges, except for neutrinos, and quarks, in addition, color charges. These charges are associated with the symmetry groups $SU(3)$ for color, $SU(2)$ for isospin and $U(1)$ for hypercharge, the average electric charge of an iso-multiplet, integrated *in toto* to the symmetry constellation $SU(3) \times SU(2) \times U(1)$. The particles are organized in three families of the same charge structures, *i.e.* they are isomorphic except for the masses; three families is the minimum for accommodating CP -violation in the Standard Model.

These particles have all been detected experimentally, and their nature, charges and masses, has been deciphered. Only the properties of the neutrinos still await clarification.

The charges of the matter particles are sources of fields which mediate the strong, electromagnetic and weak forces among the particles. The strongly interacting gluons form an octet of color fields. Mixed combinations of the isospin W -fields and the hypercharge B field build up the weak and electromagnetic force fields [1], *i.e.* the charged and neutral weak force fields W^\pm, Z^0 and the electromagnetic photon field γ . All these fields are described by gauge theories, a theoretical concept introduced to explain the laws of electromagnetism [5]. First developed for neutral force fields, like the photon, and corresponding to abelian symmetries, they have later been generalized to charged force fields, like gluons and weak fields, in non-abelian theories [6]. The concept of gauge theories builds the theoretical basis of all interactions in the Standard Model. Numerous high-precision experiments, *notabene* at LEP, have confirmed the predictions derived from the gauge symmetries [7], including the self-couplings of the color and electroweak gauge fields, which are characteristic to the non-abelian nature of symmetries.

The fourth force in nature, gravity, is not isomorphic with the above standard forces and of different structure; gravity is attached *ad hoc* as a classical element to the Standard Model.

The color force and the electromagnetic force are of long-range character and the associated field quanta, carriers of the forces, are massless, a straightforward consequence of the gauge symmetries. For quite some time, the short-range character of the weak force, connected with large masses of the weak bosons, had been a barrier for describing the weak interactions by a non-abelian gauge theory [6], a natural symmetry concept for forces carrying charges. Masses introduced by hand however destroyed the gauge symmetry and thus the very basis of this concept. The problem was solved when the concept of gauge symmetry was connected with the concept of spontaneous symmetry breaking [8], in which solutions of the field equations have a minor rank of symmetry than the equations themselves. The breakthrough for this solution was achieved in 1964 when the Higgs mechanism was intro-

duced by Englert and Brout [9], Higgs [10], and Hagen, Guralnik and Kibble [11] to generate masses for vector bosons in gauge theories. Even though different techniques were applied, the physical key role is played by massless scalar particles which emerge from theories with spontaneous symmetry breaking. While the Goldstone theorem [8] predicts these particles in theories with spontaneously broken global symmetries, they are absorbed in local gauge theories to build up the longitudinal field components and to transform the massless gauge bosons to massive states. The energy transfer to the gauge field connected with the absorption of the Goldstone boson can be re-interpreted as generating mass to the gauge fields. Since the longitudinal field component does not carry spin along the motion of the field, it can be synthesized by the spinless Goldstone boson.

This mechanism was adopted for formulating the electroweak sector of the Standard Model by Salam [2] and Weinberg [3]. Introducing a complex iso-doublet scalar field with four degrees of freedom, as a minimum, three Goldstone components of the four scalar field degrees are absorbed to provide masses to the W^\pm, Z -bosons. At the same time isospin symmetric interactions between the fermion fields and the scalar field generate the fermion masses. In providing masses to three gauge bosons, one out of the four scalar degrees of freedom is left over, manifesting itself as a real neutral scalar particle in this basic realization of electroweak symmetry breaking, the Higgs boson.

Originally introduced into the Standard Model, the Higgs mechanism, as a generic element, has been applied subsequently in a large variety of theories. They may broadly be divided into two classes. In the first class the Higgs field is a fundamental field, eventually up to energies close to the Planck scale, the scale of order 10^{19} GeV where gravity becomes strong and must be intimately connected with the particle system. A set of Higgs particles may be incorporated in the theories of this class, as required, *e.g.*, for supersymmetric theories. The second class comprises theories in which novel strong interactions, characterized by an energy scale potentially as small as TeV, trigger the spontaneous symmetry breaking. Basic technicolor theories [12], which do not include light physical scalar fields, are a characteristic paradigm of this class. Intermediate scales and light Higgs bosons identified with pseudo-Goldstone bosons are introduced in branches like Little Higgs models [13].

In succession to the “*Higgs Hunter’s Guide*”, Ref. [14], an extensive overview of electroweak symmetry breaking in general and the Higgs mechanism in particular has been presented in Ref. [15], and broad discussions of phenomenological aspects¹ can be found in Refs. [16] and [17].

1.2 Higgs in the Standard Model

The Higgs sector of the Standard Model is built up by a scalar iso-doublet field, including bilinear and quadrilinear self-interactions, in which two and four scalars, respectively, are

¹We apologize to all authors whose important work could not be given the reference proper in this very brief report.

coupled with each other. To guarantee the vacuum to be stable, the coupling λ of the quadrilinear interaction must be positive. If, on the other hand, the coefficient of the bilinear mass term is negative, a minimum is induced in the interaction energy and the ground state shifts from field-strength zero to a non-zero value v , *cf.* Fig. 1. This ground-state value is related to the Fermi coupling in the weak interactions by $v = [1/\sqrt{2}G_F]^{1/2}$, numerically 246 GeV, the fundamental electroweak scale.

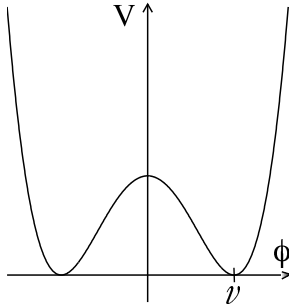


Figure 1: *Characteristic energy potential for scalar fields in theories of spontaneously broken symmetry. The ground-state (vacuum) is moved from $\phi = 0$ to a non-zero value v at the minimum of the potential.*

The interaction of the $SU(2) \times U(1)$ gauge fields with the scalar field v generates gauge-boson masses $M^2 = g^2 v^2/4$. Similarly the masses of the fermionic leptons and quarks f are generated by gauge-symmetric Yukawa interactions which couple the scalar iso-doublet with the fermion iso-doublets and iso-singlets, resulting in fermion masses $m_f = g_f v/\sqrt{2}$.

In the process of shifting the zero masses of the gauge bosons to non-zero values, three Goldstone modes of the scalar field are absorbed by the gauge bosons, leaving one physical Higgs state out of the four components of the iso-doublet scalar.

1.2.1 Higgs mass

The Higgs mass is related to the quadrilinear coupling in the Higgs potential, $M_H^2 = 2\lambda v^2$. Since the coupling λ is not pre-determined, the Higgs mass cannot be predicted. In fact, it is the, presently, only unknown parameter in the Higgs sector of the Standard Model while all other Higgs couplings to weak bosons, leptons and quarks can be related to their well measured masses.

Constraints, at the theoretical as well as experimental level, restrict the value of the Higgs mass quite strongly. A rather general bound $M_H < 700$ GeV follows from the unitarity of the theory [18], which leads, by requiring the probability for the scattering of particles to be less than unity, to an upper bound on partial-wave amplitudes in elastic WW scattering,

depending quadratically on the Higgs mass. However, this general bound is reduced considerably if additional theoretical assumptions and experimental constraints are exploited.

(a) Extrapolation to grand-unification scale

The quadrilinear Higgs coupling λ grows indefinitely with energy, driven by radiative corrections involving the Higgs self-interactions. To prevent the coupling from becoming strong before the scale of the grand unification [GUT] of the forces of the Standard Model is reached, the value at the electroweak scale must be bounded [19], and the Higgs mass is restricted correspondingly, $M_H^2 < 8\pi^2 v^2 / 3 \log(M_{GUT}^2/v^2)$. The underlying assumption of weakly interacting fields in the Standard Model up to the grand unification scale is supported by the qualitative prediction, of the electroweak mixing parameter, $\sin^2 \theta_W \sim 0.2$, when evolved from the GUT value $3/8$ down to the value at the experimental electroweak scale [20]. On the other hand, quantum corrections involving fermionic top quarks reduce the quadrilinear Higgs coupling. To prevent the coupling from falling below zero, which would render the vacuum unstable, the value at the electroweak scale must be bounded from below [19]. *In toto*, the Higgs mass of the Standard Model is restricted, including theoretical uncertainties [21], to the conservative range

$$124 \text{ GeV} < M_H < 180 \text{ GeV} \quad (1)$$

in this scenario. Otherwise new strong interactions would be predicted with a characteristic scale between the electroweak scale and the Planck scale. Uncertainties of a few GeV in the theoretical estimate of the lower limit [21] must be exhausted if the conflict of a stable vacuum with a Higgs mass value of 125 GeV, for example, should be circumvented.

(b) Electroweak radiative corrections

Support for a light Higgs mass in the Standard Model has also been derived from the high-precision measurements of the electroweak observables at LEP1, the LEP mode which operated around the Z pole, and of observables in vastly different fields from high-energy neutrino scattering down to polarization effects in atomic physics. Since the Standard Model is renormalizable [22], *i.e.* only a small number of basic parameters, masses and couplings, must be introduced in the theory as experimental observables, quantum corrections can be predicted to high accuracy. The Fermi coupling G_F , at the Born level $\sim \alpha / \sin^2 2\theta_{eff}^{lept} M_Z^2$, is affected by quantum corrections logarithmically in the Higgs mass [23], $\sim \alpha \log M_H^2 / M_W^2$. They add to corrections quadratic in the top-quark mass (which had been exploited, in fact, to predict this mass successfully before top quarks were detected experimentally in $p\bar{p}$ collisions). Since all the parameters in G_F were measured at LEP1 very precisely, in particular the Z -boson mass and the effective mixing parameter $\sin^2 \theta_{eff}^{lept}$, the Higgs mass can be constrained from the experimental data. The result of the global analysis [24], which is displayed in Figure 2, can be condensed to the estimates

$$\begin{aligned} M_H &= 92_{-26}^{+34} \text{ GeV} \\ &\leq 161 \text{ GeV (95\% CL)} \end{aligned} \quad (2)$$

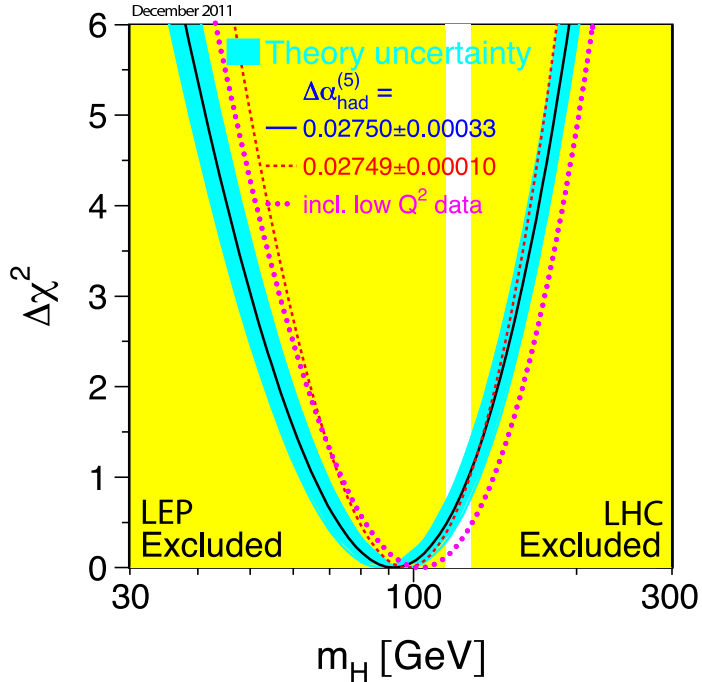


Figure 2: Estimate of the Higgs mass in the Standard Model from electroweak precision measurements [24]. The excluded area labeled LHC has been updated with results from Ref. [51], courtesy M. Grünwald. Present search limits for the Higgs boson from LEP and LHC leave only a small mass gap, the white bar close to the minimum of the χ^2 distribution.

for expectation value and upper limit of the Higgs mass in the Standard Model, to be confronted with direct experimental searches.

Thus the GUT-based argument as well as the evaluation of the quantum (radiative) corrections, largely based on LEP1 measurements, generate a consistent picture for a light Higgs boson within the Standard Model.

1.2.2 Higgs decay modes and production mechanisms

Conform with the target of the Higgs mechanism, the couplings of the Higgs boson to pairs of massive gauge bosons and fermions will be of the order of their masses: $g_H \sim M_V, m_f$. This rule gives rise to a characteristic set of potential production channels in e^+e^- collisions, and in $p\bar{p}$ and pp collisions. Likewise the hierarchy of the decay modes is dictated by this mass rule.

(a) Decay modes of the Higgs boson

The decay modes define the mass-dependent signatures in searches for the Higgs bosons. The

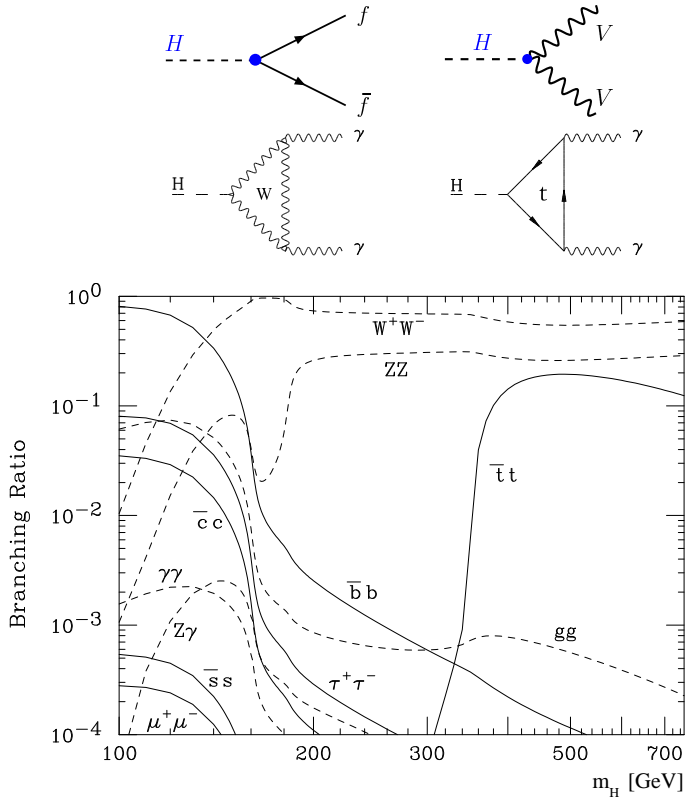


Figure 3: Branching ratios for Higgs decay modes [15]. On top: diagrams exemplifying important channels, fermion $f\bar{f}$, vector boson $VV = ZZ, WW$ and loop-induced photon $\gamma\gamma$ decay pairs.

particle with the largest mass kinematically allowed for pair decay provides the dominant decay mode, reversed however, by statistics, in the W, Z sector and supplemented by photonic (and other) loop decays:

$$H \rightarrow b\bar{b}, \tau^+\tau^-; W^+W^-, ZZ; \dots \quad (3)$$

$$H \rightarrow \gamma\gamma. \quad (4)$$

The branching ratios for the main decay channels are shown in Figure 3. Decays to electroweak W, Z -bosons are effective already significantly below the pair thresholds, with one of the bosons being virtual. The Higgs coupling to photons is mediated by W -boson and t -quark loops, as exemplified in the diagrams on top of Fig. 3.

The total width of the Higgs boson remains narrow throughout the low-mass range, rising from a few MeV near 120 GeV to about 1 GeV at the ZZ threshold. Thus, the width in this mass range is below the experimental resolution.

For Higgs decays to final states without multiple neutrinos and with sufficient background control, the Higgs boson can fully be reconstructed. Most attractive modes, particularly in

the LHC environment, are the $\gamma\gamma$ decays at low Higgs masses and the $ZZ \rightarrow \ell\ell\ell\ell$ channel at medium to large masses. These final states generate resonance peaks above smooth backgrounds, thus allowing the Higgs reconstruction in a model-independent way – the classical procedure for a particle as fundamental as the Higgs boson.

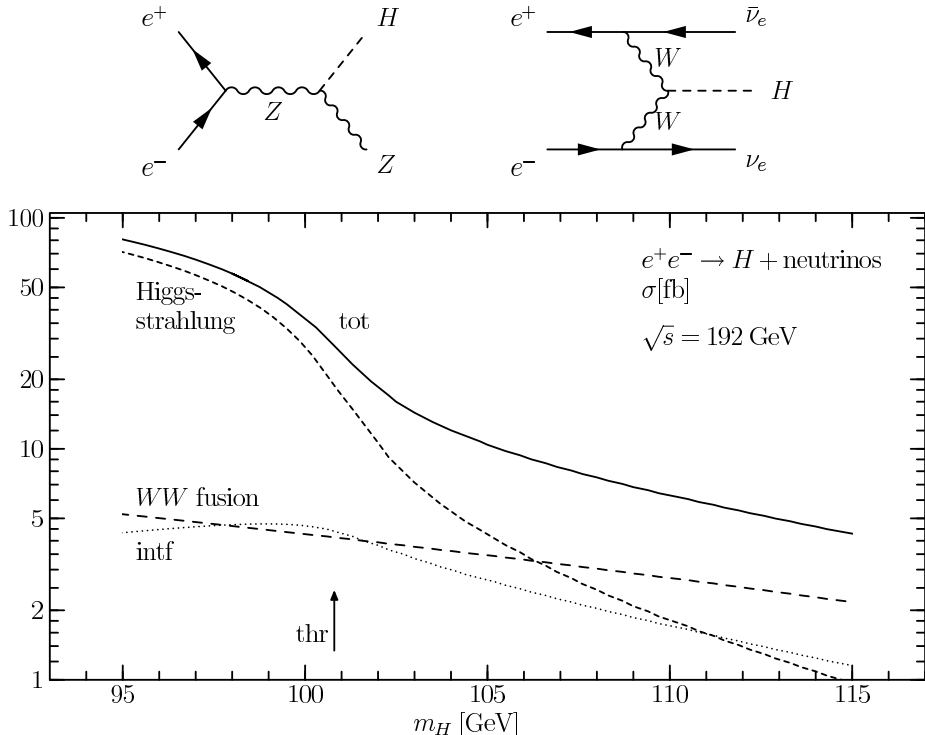


Figure 4: Higgs production cross section $\sigma[e^+e^- \rightarrow H\bar{\nu}\nu]$ [28]. The total cross section is built up by Higgs-strahlung HZ with Z decaying to neutrinos, WW fusion and their interference ($intf$). Higgs-strahlung falls off rapidly above the threshold (thr) region. Other than $\bar{\nu}\nu$ final states in Higgs-strahlung can be derived from the short-dashed curve by re-adjusting the Z -decay branching ratio properly. Diagrams on top describe the Higgs-strahlung and the vector-boson fusion mechanism for Higgs production in e^+e^- collisions.

(b) Higgs production in e^+e^- collisions

Four processes, primarily, have been exploited at LEP to search for Higgs bosons [25–28] without gap from zero-mass up to masses above the Z -boson:

$$\begin{aligned} \text{LEP1 : } & \text{Bjorken process } Z \rightarrow H + [Z] \rightarrow H + f\bar{f} \\ & \text{Radiative process } Z \rightarrow H + \gamma \end{aligned} \quad (5)$$

$$\begin{aligned} \text{LEP2 : } & \text{Higgs-strahlung } e^+e^- \rightarrow [Z] \rightarrow H + Z \\ & W\text{-fusion} \quad e^+e^- \rightarrow [WW] + \bar{\nu}_e\nu_e \rightarrow H + \bar{\nu}_e\nu_e, \end{aligned} \quad (6)$$

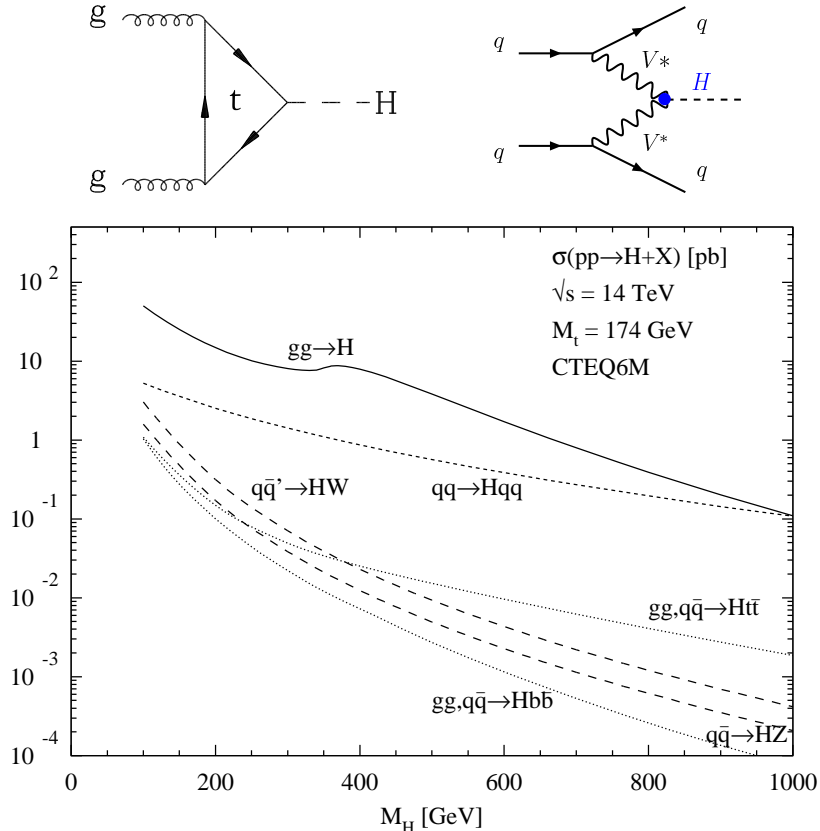


Figure 5: The Higgs production channels at the LHC [15]. The value of the top mass M_t affects the cross sections for gluon fusion and Higgs bremsstrahlung off top-quark pairs; gluon and quark densities are adopted from parametrizations of CTEQ6M. On top: gluon fusion [29–33] and weak boson fusion [34], two central mechanisms for producing Higgs bosons at LHC; the projectiles, gluons and quarks, as fundamental constituents, each carry major fractions of the proton energies.

the square brackets representing virtual states; additional channels, like $[ZZ]$ fusion, have been of minor impact. While the Higgs boson is coupled to the heavy Z, W^\pm -bosons directly, the coupling to the $Z\gamma$ final state is mediated by virtual W^\pm -bosons and top quarks. The branching ratios of the Bjorken process and the radiative process, and the production cross sections in Higgs-strahlung and Higgs W -fusion are large enough, *cf.* Figure 4, to cover the entire range from zero Higgs mass up to the kinematical limit of Higgs-strahlung: $0 < M_H < E_{ee}^{tot} - M_Z$.

(c) Higgs production in pp and $p\bar{p}$ collisions

The production channels of Higgs bosons in pp collisions at the LHC, and $p\bar{p}$ collisions at the Tevatron, parallel the LEP2 channels after leptons are replaced by quarks, spearheaded

however by the gluon-fusion mechanism [29–33]:

$$\begin{aligned}
\text{Higgs-strahlung} &: q\bar{q} \rightarrow [W] \rightarrow H + W \quad [\text{and } W \rightarrow Z] \\
W\text{-fusion} &: qq \rightarrow [WW] + qq \rightarrow H + qq \quad [\text{and } W \rightarrow Z] \\
\text{top bremsstrahlung} &: gg, qq \rightarrow t\bar{t} + H \\
\text{gluon-fusion} &: gg \rightarrow H,
\end{aligned} \tag{7}$$

The gluons are connected with the Higgs boson by a triangular top-quark loop in the gluon-fusion process. The experimental cross sections are derived by summing the subprocesses over all quark and gluon parton-densities. Controlling of the QCD radiative corrections is particularly important for the gluon-fusion process. Next-to-leading order corrections [30] raise the cross section by almost a factor 2 compared to the original leading-order approach [29]; while, similar to the electroweak corrections [31], the two-loop order [32] gives rise to a modest additional increment, three-loop corrections [33] finally remove residual scale artifacts which are present when the expansion is truncated at low orders.

An overview of the production cross sections for the Higgs bosons in the channels listed above, is displayed in Figure 5. For an integrated luminosity $\mathcal{L} = 100 \text{ fb}^{-1}$, the production of a large number, more than 1 million, light Higgs bosons is theoretically predicted in the Standard Model.

1.3 Extended systems

Spontaneous symmetry breaking has been implemented in a large variety of mechanisms for generating the masses of electroweak gauge bosons and fermions. Motivated by the successful estimate of the electroweak mixing parameter $\sin^2 \theta_W$, particular attention has been paid to theories in which the fields remain weakly interacting up to energy scales close to the grand unification scale. Supersymmetric theories are the basic paradigm of this class of theories. The opposite extreme are theories in which spontaneous symmetry breaking is triggered by new strong interactions near the TeV energy scale, eventually including composite Higgs bosons. This mechanism has been incorporated first in technicolor theories, developed to wider branches later.

1.3.1 Supersymmetry

Supersymmetry [35], a novel symmetry scheme in which fermionic partners are associated with the bosonic fields and *v.v.*, is tightly connected with the Higgs mechanism. In theories in which the fields remain weakly interacting up to the GUT scale, quantum corrections would generally drive scalar masses [36] to values close to this scale, $M_H^2 \sim \alpha M_{GUT}^2$. In supersymmetric theories [susy] the fermionic and bosonic corrections however cancel each other, as a consequence of the Pauli principle, up to the mass gap between the two types of

states, *i.e.* $M_H^2 \sim \alpha(M_{susy}^2 - M_{SM}^2)$. Neglecting the small standard masses M_{SM} of the Standard Model, for low Higgs masses near M_Z the masses of supersymmetric partners should therefore not exceed the scale $M_{susy} < \mathcal{O}(1 \text{ TeV})$.

To guarantee the theory to be supersymmetric, the Higgs iso-doublet of the Standard Model must at least be doubled. The doubling expands the number of real Higgs states to five: three neutral particles and one pair of charged particles [37]. Since the quadrilinear coupling in the Higgs potential of the minimal theory is set by the square of the gauge couplings, the mass of the lightest neutral particle h^0 , after including radiative corrections of the order of $G_F m_t^4$, is predicted [38] to be small, about

$$M_{h^0} < 135 \text{ GeV}, \quad (8)$$

while the masses of the remaining particles $\{H^0, A^0, H^\pm\}$ may have values anywhere between the electroweak scale and $\mathcal{O}(\text{TeV})$.

The production cross sections of the lightest Higgs boson h^0 for Higgs-strahlung and W -fusion in e^+e^- collisions are reduced, $\sim \sin^2(\alpha - \beta)$, in relation to the Standard Model by the mixing of Higgs states among themselves (angle α) and with Goldstone states (angle β) [37]. The suppression is balanced partly, however, by the additional pair-production channel $e^+e^- \rightarrow h^0 A^0$ of size $\sim \cos^2(\alpha - \beta)$. Similarly for LHC production processes. For the mixing parameter $\tan \beta$ sufficiently large, Higgs bremsstrahlung off b -quarks, produced pairwise at LEP and LHC, provides another potentially copious source of Higgs bosons.

While supersymmetry solves the problem to keep Higgs masses low in weakly interacting theories in a natural way, large supersymmetry scales, as signaled by rising bounds on masses of supersymmetric particles, indicate however another, yet much less severe problem. In the minimal supersymmetric standard model, the supersymmetric Higgs mass parameter μ and the mass parameters M_k breaking supersymmetry in the scalar sector, both of TeV size, must nearly cancel each other, though being of unrelated origin, to generate the small electroweak scale, $\frac{1}{2}M_Z^2 \simeq c_k M_k^2 - \mu^2$. Extending the minimal supersymmetric model by additional Higgs fields, iso-scalars for example, can ease the problem. Thus, the Higgs sector in supersymmetry may have a rather complex structure.

1.3.2 Strong electroweak symmetry breaking

Spontaneous symmetry breaking is a well established concept in strong interactions, giving rise to zero-mass pions if small quark masses are neglected. Introducing new strong technicolor interactions, in parallel to QCD but at a high scale $\Lambda_{TC} \sim \text{TeV}$ [12], will lead, in analogy, to Goldstone bosons, massless bound states of new fermions, which are absorbed by electroweak gauge bosons to generate non-zero masses, $M^2 = g^2 f^2 / 4$ with $f = v$. This mechanism does not incorporate any light Higgs particles *sui generis*, but physical scalar masses are in general of size TeV. Interactions between W, Z bosons become strong at TeV

energies, affecting the predictions for quasi-elastic WW scattering amplitudes [39]. Fermion masses demand the systematic extension of the theory. Dynamical solutions, which deviate, as suggested in walking technicolor, from the standard QCD path, are required however to reconcile the theory with the observed suppression of flavor-changing processes and the precision measurements at LEP.

Two scales characterize technicolor theories, the technicolor scale Λ_{TC} and the scale characterizing spontaneous symmetry breaking which coincides with the electroweak scale v . This concept can accommodate also light Higgs bosons if the theories are extended in a form as realized in Little Higgs Models [13]. Introducing new strong interactions at a scale Λ_* of 10 TeV or beyond, the spontaneous breaking of a global symmetries associated with the new interactions gives rise to a large set of Goldstone bosons in addition to the standard iso-doublets. Gauge symmetries of the theory extended beyond the standard gauge group are broken at the same time, leading to new gauge bosons at the TeV scale. Quantum corrections endow most of the Goldstone bosons with masses of order TeV, while the standard iso-doublet Higgs boson will acquire mass only by multiple quantum corrections, generating the small standard electroweak scale v . Thus, in addition to the spectrum of the Standard Model including only one light Higgs boson, models of this type generate extended spectra of new gauge bosons and Higgs bosons, as well as fermions, at the TeV scale, which can be searched for at the LHC [40].

Aspects of technicolor models can be connected with extra space dimensions [41, 42]. The fifth components of the gauge fields in theories, in which 4-dimensional space-time is extended by a new space dimension, can be identified with the scalar fields. Proper boundary conditions on the gauge fields in the extra dimension generate electroweak symmetry breaking. The experimental observation of Kaluza-Klein states in the TeV energy range at LHC, coming with the compactification of the five dimensions to the standard four space-time dimensions, would open the gate to this scenario of electroweak symmetry breaking.

2 Experimental Results

The search for the neutral Higgs boson in the Standard Model was an integral part of the physics programme of the four LEP collaborations, ALEPH, DELPHI, L3 and OPAL, from the running of LEP at the Z pole (LEP1) up to the highest centre-of-mass energies, in particular from 206 GeV to 209 GeV (LEP2).

Data collected by the four LEP collaborations prior to the year 2000 gave no direct indication of the production of the Standard Model Higgs boson [43] and excluded masses from zero up to a lower bound of 107.9 GeV (at 95% confidence level). During the last year of the LEP programme, substantial data samples were collected at centre-of-mass energies

exceeding 206 GeV, extending the search sensitivity to Higgs boson masses of about 115 GeV through the Higgs-strahlung process $e^+e^- \rightarrow HZ$ (see Eq.(6)) and providing one of the most stringent limits for the Higgs mass.

After the final results from the four collaborations were published individually [46], a LEP-wide combination was performed in order to increase the overall sensitivity of the searches for a possible Higgs boson signal. The result is published in [44] and is summarized here ². The data were collected for centre-of-mass energies from 189 GeV to 209 GeV corresponding to a total integrated luminosity of $\approx 2.5 \text{ fb}^{-1}$.

2.1 Standard-Model Higgs boson search

2.1.1 Search procedures

At LEP energies, the Standard-Model Higgs boson would be produced mainly in association with the Z boson through the Higgs-strahlung process $e^+e^- \rightarrow HZ$. This process is supplemented by a small contribution from the W -fusion, which produces a Higgs boson and a pair of neutrinos in the final state (see Eq.(6) and Figure 4). As illustrated in Figure 3 for masses below 115 GeV the Higgs boson would decay mainly into $b\bar{b}$ quark pairs with a branching ratio of 74% while decays to $\tau^+\tau^-$, W^+W^- , $gg \approx 7\%$ each, and $c\bar{c} \approx 4\%$ constitute the rest of the decay width. The dominant final-state topologies are b -jets, quark jets and lepton pairs as produced in the following channels:

- four jet final state ($H \rightarrow b\bar{b}$)($Z \rightarrow q\bar{q}$),
- leptonic final states ($H \rightarrow b\bar{b}$)($Z \rightarrow \ell^+\ell^-$), where ℓ denotes charged leptons e, μ, τ ³,
- missing energy final state ($H \rightarrow b\bar{b}$)($Z \rightarrow \nu\bar{\nu}$).

Background from two-photon processes and from the radiative return to the Z boson, $e^+e^- \rightarrow Z\gamma(\gamma)$ fermion pairs and WW or ZZ production is effectively reduced by selective cuts and the application of multivariate techniques such as likelihood analyses and neural networks. The identification of b -quarks in the decay of the Higgs boson, by secondary vertices for instance, is essential in the discrimination between signal and background. The details of these analyses by the four experiments are given in [46]. In Figure 6 an example of a candidate event from one of the LEP experiments in the four-jet channel (a $b\bar{b}$ pair together with a $q\bar{q}$ pair) is shown.

The data from the four experiments are combined using subsets of specific final-state topologies or of data sets collected at different centre-of-mass energies. Essentially, two variables are used to statistically discriminate between signal and background events.

²For this combination a special working group was created by the four Collaborations [45].

³Tau pairs can also contribute through the ($H \rightarrow \tau^+\tau^-$)($Z \rightarrow q\bar{q}$) final state.

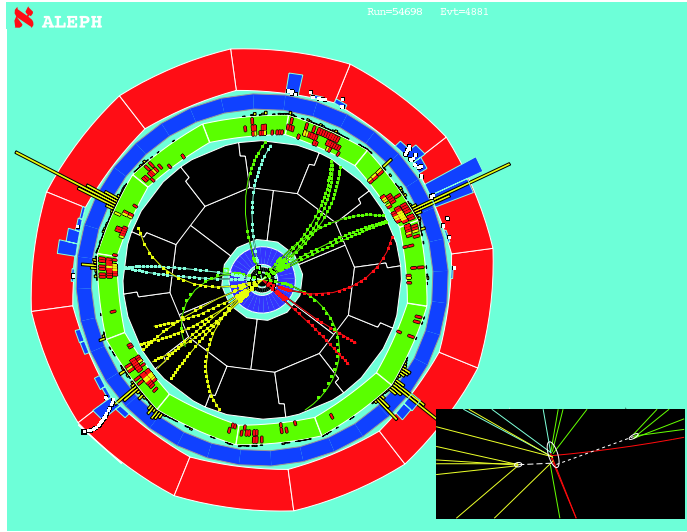


Figure 6: Four-jet event, shown in the view transverse to the beam. The insert shows a closeup of the charged particles at the interaction region. Two secondary vertices are clearly reconstructed, consistent with two decaying b -quark particles.

The most discriminating variable is the reconstructed Higgs boson mass m_H^{rec} , in the distribution of which the signal events would accumulate around the real Higgs boson mass. In Figure 7 the observed distributions together with the expectations are shown for illustration at two levels of signal purity. Reasonable agreement of the data with the expected background is observed. The enhancement in the vicinity of the Z boson mass is from the $ee \rightarrow ZZ$ background process. However, for Higgs boson production close to the kinematic threshold, only few events are expected and therefore a higher level of discrimination is needed.

The second variable used in the analysis combines many discriminating event features which allow to distinguish on a statistical basis between signal and background events. The most important of these variables describes the identification of a b -quark which appears in all Higgs search channels (see above). This information is combined with other event features like multivariate tests, likelihood functions or neural networks, leading together to the second discriminating variable that is used in the combined analysis.

2.1.2 Hypothesis testing

The combined LEP dataset is tested for compatibility with two hypotheses: the background-only scenario and the signal-plus-background scenario. The two discriminating variables described in the previous section are used to calculate the likelihoods ratio

$$Q = L_{s+b}/L_b \quad (9)$$

which is defined with the likelihood functions L_{s+b} and L_b given by the probability density function of the two hypotheses evaluated at the data points. For convenience, the logarithmic

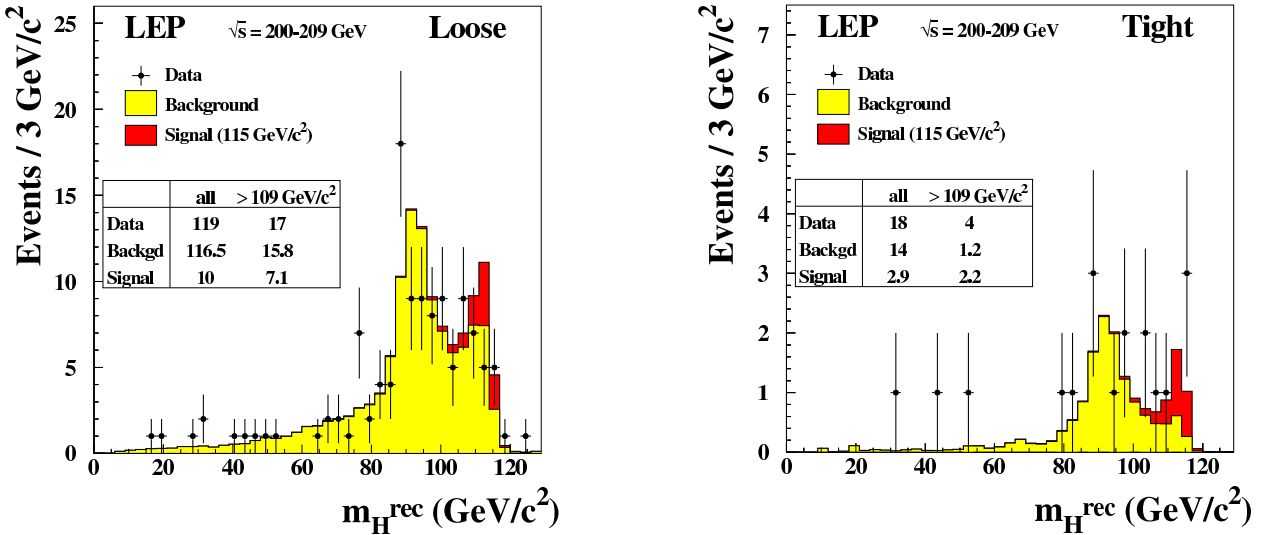


Figure 7: Distributions of the reconstructed Higgs boson mass for two selections with different signal purities. Superimposed to the data (dots) are the Monte Carlo predictions (histograms), lightly shaded for the background, heavily shaded for a Higgs boson of mass 115 GeV. In the loose and tight selections the cuts are adjusted in such a way as to obtain, for a Higgs boson of mass 115 GeV, approximately 0.5 or 2 times more expected signal than background events when integrated over the region $m_H^{\text{rec}} \geq 109$ GeV [44].

form $-2 \ln Q$ is used as the test statistic since this quantity is approximately equal (exactly equal in the limit of high statistics) to the difference in χ^2 when the observed distribution in the two variables is compared to that expected on the basis of simulations for the two hypotheses.

In Figure 8 the likelihood test $-2 \ln Q$ is shown as a function of the hypothesized Higgs boson mass M_H .

Values of $-2 \ln Q$ larger than zero correspond to a likelihood ratio less than one, *i.e.* the likelihood for the signal-plus-background hypothesis is smaller than the one for background only. The small negative values of $-2 \ln Q$ above 114 GeV indicate that the hypothesis including a Standard Model Higgs boson of such a mass is slightly more favoured than the background hypothesis. Also, the median expectation for the signal-plus-background hypothesis converges to the observation in this mass range.

The compatibility of a data set with a hypothesis is quantified by the confidence level CL. Here, CL is the probability of obtaining in simulated measurements a likelihood ratio, as defined above, smaller than the one observed with the data. If CL_b is the confidence level for the compatibility of the data in a Higgs search with the background-only hypothesis, the p -value [47], $p = 1 - \text{CL}_b$, is, correspondingly, the probability to obtain a configuration of events which is less background-like than the one observed. A signal would produce an excess relative to the background, which would appear as a dip in $1 - \text{CL}_b$.

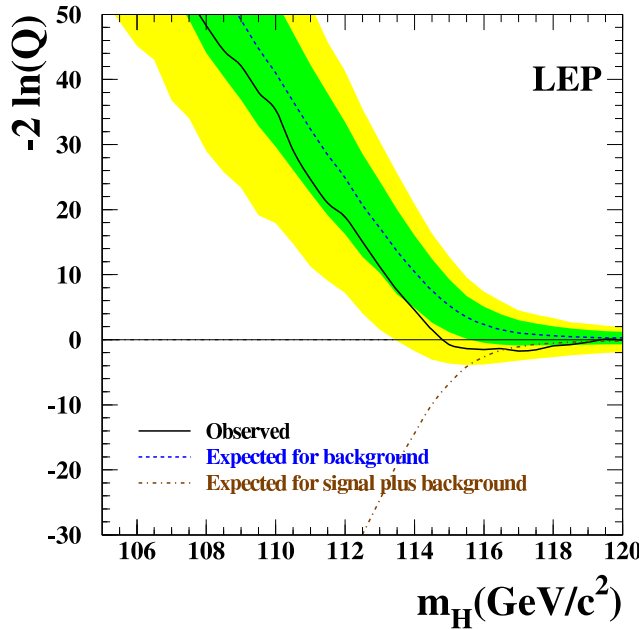


Figure 8: The log-likelihood estimator $-2 \ln Q$ as a function of the Higgs boson mass. The full curve represents the observation; the dashed curve shows the median background expectation; the dark and light shaded bands represent the 68% and 95% probability bands about the median background expectation. The dash-dotted curve indicates the position of the minimum of the median expectation for the signal-plus-background hypothesis [44].

Figure 9 shows the background confidence $1 - \text{CL}_b$ for M_H in the range from 80 to 120 GeV. The dip in the region $M_H \approx 98$ GeV corresponding to 2.3 standard deviations, cannot be interpreted as coming from the Standard Model Higgs boson. The number of signal events which would produce such a deviation from the background expectation is about an order of magnitude smaller than the number expected for a Standard Model Higgs boson. In the region of $M_H \approx 115$ GeV the dip is compatible with the Standard Model Higgs boson hypothesis but its significance is only of 1.7 standard deviations.

The dash-dotted line in Figure 9 shows the position of the minimum of the median expected $1 - \text{CL}_b$ for the signal-plus-background hypothesis. This line indicates the depth of the dip that would result from a Standard Model Higgs boson of mass M_H .

2.1.3 Higgs mass limit

Similarly, one can also quantify the compatibility of the observation with the signal-plus-background hypothesis, CL_{s+b} . The confidence level ratio $\text{CL}_s = \text{CL}_{s+b}/\text{CL}_b$ is a function of the test mass and is used to derive a lower bound on the Standard Model Higgs boson mass (Figure 10). The lowest mass giving $\text{CL}_s = 0.05$ is taken as the lower bound at the 95%

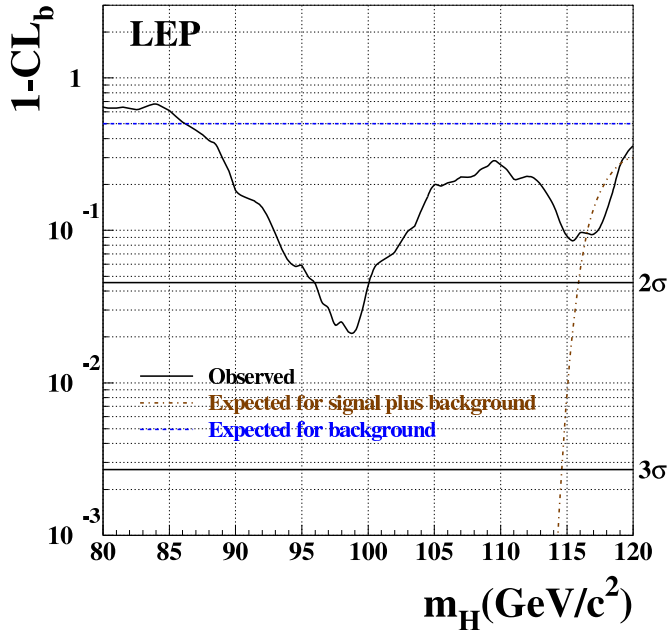


Figure 9: The background confidence $1 - \text{CL}_b$ as a function of the test mass M_H . Full curve: observation; dashed curve: expected background confidence; dash-dotted line: the position of the minimum of the median expectation of $1 - \text{CL}_b$ for the signal-plus-background hypothesis, when the signal mass indicated on the abscissa is tested. The horizontal solid lines indicate the levels for 2σ and 3σ deviations from the background hypothesis [44].

confidence level. The observed 95% CL lower bound on the mass of the Standard Model Higgs boson obtained from LEP data is 114.4 GeV while the expected 95% CL is 115.3 GeV.

2.1.4 Towards the LHC

After the closure of the LEP collider, the search for the Higgs boson was continued at the Fermilab Tevatron $p\bar{p}$ collider. The cross section for the production of the Standard Model Higgs boson in $p\bar{p}$ collisions is close to 1 pb for low masses. The two experiments, CDF and D0, have not observed any excess and exclude the region of $156 \text{ GeV} \leq M_H \leq 177 \text{ GeV}$ at 95% CL [48].

Since 2010, the CERN pp collider LHC is in operation, in the first phase with an energy of 7 TeV, to be extended later to 14 TeV. Hence the focus of the Higgs boson search has moved to the two large detectors ATLAS and CMS [49, 50]. They have been optimized for the Higgs boson search in a mass range from the LEP limit of 114.4 GeV up to ≈ 700 GeV. In pp collision the Standard Model Higgs boson production is dominated by gluon-gluon fusion (Figure 5) with a large cross section of tens of pb.

The dominant Higgs decay mode below ≈ 140 GeV is $H \rightarrow b\bar{b}$, and above ≈ 140 GeV

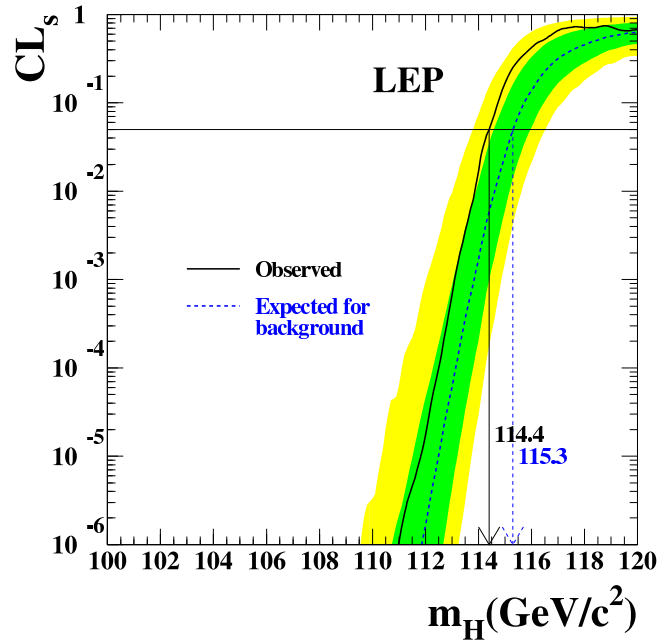


Figure 10: The ratio $CL_s = CL_{s+b}/CL_b$ for the signal-plus-background hypothesis. Solid line: observation; dashed line: median background expectation. The dark and light shaded bands around the median expected line correspond to the 68% and 95% probability bands. The intersection of the horizontal line for $CL_s = 0.05$ with the observed curve is used to define the 95% confidence level lower bound on the mass of the Standard Model Higgs boson [44].

it is $H \rightarrow WW$ (and ZZ). However, for a mass below 130 GeV the most sensitive channel in terms of signal to background discrimination is the $H \rightarrow \gamma\gamma$ final state despite its low branching ratio of $\approx 2 \times 10^{-3}$. Above 130 GeV the $H \rightarrow WW$ and $H \rightarrow ZZ$ final states dominate. At high masses the $H \rightarrow ZZ$ mode with each Z decaying to an e^+e^- or $\mu^+\mu^-$ pair is the cleanest channel. Irreducible backgrounds in the most sensitive final states WW , ZZ and $\gamma\gamma$ are from $q\bar{q}$ annihilation processes.

On December 2011 ATLAS and CMS reported in a special seminar at CERN [51] the status on the Higgs boson search based on data collected by each experiment corresponding to an integrated luminosity of about 5 fb^{-1} . The main result is that the Standard Model Higgs boson, if it exists, is most likely to have a mass constrained to the range

115.5 – 131 GeV (ATLAS)

115 – 127 GeV (CMS).

Intriguing hints have been seen by both experiments in the mass range of 124 - 126 GeV, in particular in the $H \rightarrow \gamma\gamma$ channel. However, the excess in both experiments is not strong enough to claim a discovery. Hence, the hunt for the Higgs boson will continue at the LHC during 2012.

With high luminosity at the LHC, the experiments have the potential to fully cover the mass range for the Standard-Model boson search.

2.2 Supersymmetry

In supersymmetric theories, like the Minimal Supersymmetric Standard Model MSSM, the lightest of the neutral Higgs bosons, h^0 , is naturally predicted to have a mass less than ≈ 135 GeV (see chapter 1.3.1). This prediction provided a strong motivation for the searches at LEP energies. The masses of the other CP -even and odd neutral and charged bosons Higgs bosons H^0, A^0, H^\pm in the MSSM (and supersymmetric theories in general) may be as large as $\mathcal{O}(1 \text{ TeV})$, the typical mass scale of supersymmetric theories.

Like for the Standard Model Higgs boson search, Higgs searches in supersymmetric theories were performed by the four LEP Collaborations, including all LEP2 data up to the highest energy of 209 GeV. The combined LEP data [52] show no significant signal for Higgs boson production, neither in Higgs-strahlung processes $e^+e^- \rightarrow Zh^0/H^0$ nor in associated neutral or charged pair production $e^+e^- \rightarrow A^0h^0/H^0, H^+H^-$. These null results are used to set upper bounds on topological cross sections for a number of Higgs-like final states. Furthermore, they are interpreted in a set of representative MSSM benchmark models [53], with and without CP -violating effects in the Higgs sector.

Here, as a characteristic example the $m_h - \text{max}$ scenario [54] of the MSSM has been chosen for illustration where the stop mixing parameter is set to a large value, $X_t = 2M_{\text{susy}}$. This model is designed to maximize the theoretical upper bound on the h^0 mass within the MSSM for a given mixing parameter $\tan\beta$ and fixed top and supersymmetry mass parameters, M_t and M_{susy} . The model thus provides the largest parameter space in the h^0 direction and conservative exclusion limits for $\tan\beta$. The exclusion contours from the LEP2 combination for the MSSM are shown in Figure 11 (Ref. [52]) for the lightest Higgs boson mass M_{h^0} and the mixing parameter $\tan\beta$.

The lower bound for the mass of the charged Higgs bosons M_{H^\pm} has been set at LEP to about 78.6 GeV, significantly below the beam energy as the cross section for scalar pair production is suppressed near threshold. Similar bounds of 92.8 and 93.4 GeV apply to the masses of the heavy CP -even and odd neutral Higgs bosons M_{H^0, A^0} , respectively, depending on the mixing parameter, *cf.* [17] for details.

After accumulating high integrated luminosity at LHC, the MSSM Higgs sector can be observed in the production of the lightest Higgs boson h^0 and the heavy Higgs bosons H^0, A^0, H^\pm up to 1 TeV. The discovery of the entire spectrum of five Higgs bosons is possible only in part of the MSSM parameter space.

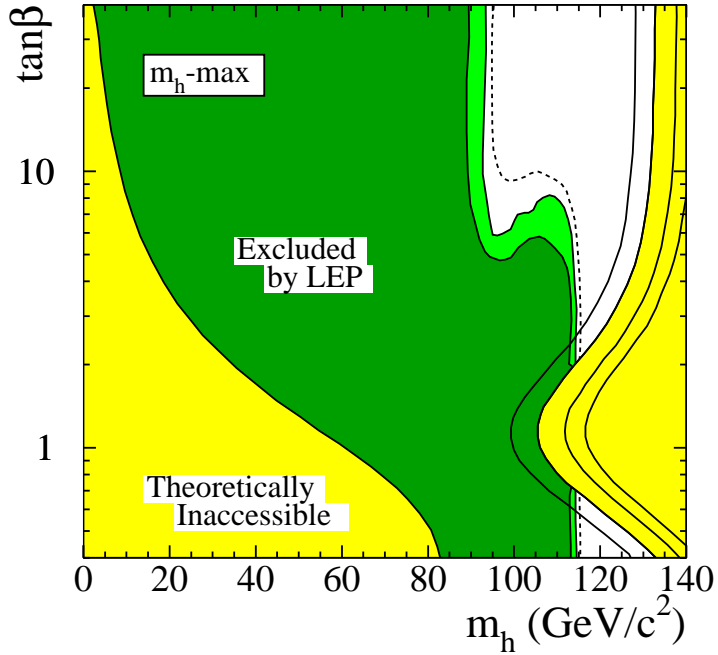


Figure 11: MSSM exclusion contours at 95% CL (light shading) and 97% (dark shading) as a function of $\tan\beta$ and lightest Higgs boson mass M_h [52].

3 Résumé

Even though the Higgs bosons of the Standard Model or related extended theories have not been discovered at LEP, while the search continues fervently at LHC, experiments at the colliders could constrain the Higgs sector [9–11], as potentially realized in nature, quite strongly.

Evaluating quantum corrections connected with high precision measurements at LEP, SLC in Stanford and the Tevatron collider, restricts the mass of the Higgs boson in the Standard Model [24] to values

$$\begin{aligned}
 M_H &= 92^{+34}_{-26} \text{ GeV} \\
 &\leq 161 \text{ GeV (95\% CL)}
 \end{aligned} \tag{10}$$

Thus, small values are suggested for the mass if the Higgs boson is realized as a fundamental particle. Likewise, this observation is compatible with values of the lightest Higgs-boson mass in supersymmetric extensions of the Standard Model. By contrast, technicolor in its simplest realization as a high-scale copy of QCD could be proven not compatible with the high-precision data. Complex constructs would be needed if electroweak symmetry breaking were triggered by novel strong interactions.

Direct searches for Higgs bosons in Z -decays at LEP1 and, primarily in the Higgs-strahlung process $e^+e^- \rightarrow HZ$ at LEP2, have ruled out, on the other hand, the mass range [44] from zero up to the 95% CL bound of

$$M_H \geq 114.4 \text{ GeV} \quad (11)$$

so that only a small gap has been left open by LEP. Correspondingly, large areas of parameter spaces in extended theories, as suggested by supersymmetry for instance, have been ruled out by the negative outcome of LEP searches.

The ATLAS and CMS collaborations at LHC have recently reduced the upper limit of the Higgs mass in the intermediate range of the Standard Model considerably [51] compared with the limit derived from electroweak precision measurements. After excluding Higgs bosons in the high mass range up to 453/600 GeV at ATLAS/CMS, with a small cut-out in the first experiment, only a very narrow gap, *cf.* Fig.2, is left open, at the time of writing, for the Higgs mass in the intermediate range,

$$115.5/115 \text{ GeV} - 131/127 \text{ GeV} \text{ at ATLAS/CMS.} \quad (12)$$

Intriguing hints have been observed by both experiments [51] in the mass range of 124 - 126 GeV, particularly in the resonating $H \rightarrow \gamma\gamma$ channel. Though the excess in both experiments is presently not strong enough to claim a discovery, the coming year 2012 can reasonably be expected to lead us to the final decision.

This gap is close to the minimum of the χ^2 distribution in Fig. 2 describing the predictions for the Higgs mass derived from high precision experiments – a potential triumph of the Standard Model.

With high luminosity at the LHC, the experiments have the potential to cover also the entire large Higgs mass range of the Standard-Model. They also exhaust the minimal supersymmetry parameter space by observing the production of the light h^0 , and H^0, A^0, H^\pm up to 1 TeV, though the complete spectrum of five states may only be accessible in part of the parameter space.

Within the framework of the Standard Model LHC covers the entire mass range possible for the Higgs boson. In this way, the closure of the Standard Model as a renormalizable theory including only a few basic parameters can be achieved or falsified. The outcome of the LHC experiments will decide whether electroweak symmetry is broken in a weakly coupled fundamental Higgs sector or, potentially, through spontaneous symmetry breaking by novel strong interactions. Each realization suggests extensions of the Standard Model either in a sector of fundamental fields, for which supersymmetry is the preferred paradigm, or in a sector of new strong interactions. In any case, perspectives of new structures in nature are opened at small distances by unraveling experimentally the mechanism of electroweak symmetry breaking.

Acknowledgements

Communications with J. Erler, D. Haidt, W. Kilian, M. Krämer, M. Spira and D. Zerwas are gratefully acknowledged, likewise diagrams adopted from A. Djouadi. Special thanks go to P. Igo-Kemenes, former convener of the LEP Higgs Working Group, for valuable remarks on the manuscript, and to M. Grünwald for providing us with the new version of the Blue-Band-plot including the most recent LHC exclusion bounds for the Higgs mass in the Standard Model. We also thank the editor, Professor H. Schopper, for the invitation to this report and his continuous advice.

References

- [1] S. L. Glashow, Nucl. Phys. **22** (1961) 579.
- [2] A. Salam, *In the Proceedings of 8th Nobel Symposium, Lerum, Sweden, 19-25 May 1968*, pp 367-377.
- [3] S. Weinberg, Phys. Rev. Lett. **19** (1967) 1264.
- [4] M. Gell-Mann, Phys. Lett. **8** (1964) 214; G. Zweig, CERN preprint TH-401 (1964); H. Fritzsch and M. Gell-Mann, eConf **C720906V2** (1972) 135 [arXiv:hep-ph/0208010]; D. J. Gross and F. Wilczek, Phys. Rev. Lett. **30** (1973) 1343; H. D. Politzer, Phys. Rev. Lett. **30** (1973) 1346.
- [5] H. Weyl, Sitzungsber. Preuss. Akad. Wiss. Berlin (Math. Phys.) **1918** (1918) 465; and Z. Phys. **56** (1929) 330; F. London, Z. Phys. **42** (1927) 375; V. Fock, Z. Phys. **39** (1926) 226.
- [6] C. N. Yang and R. L. Mills, Phys. Rev. **96** (1954) 191.
- [7] J. Erler and P. Langacker *in* K. Nakamura et al. (Particle Data Group), J. Phys. **G37**, 075021 (2010).
- [8] J. Goldstone, Nuovo Cim. **19** (1961) 154.
- [9] F. Englert and R. Brout, Phys. Rev. Lett. **13** (1964) 321.
- [10] P. W. Higgs, Phys. Lett. **12** (1964) 132; Phys. Rev. Lett. **13**, 508 (1964); Phys. Rev. **145** (1966) 1156.
- [11] G. S. Guralnik, C. R. Hagen and T. W. B. Kibble, Phys. Rev. Lett. **13** (1964) 585.
- [12] S. Weinberg, Phys. Rev. D **19** (1979) 1277; L. Susskind, Phys. Rev. D **20** (1979) 2619.

- [13] N. Arkani-Hamed, A. G. Cohen and H. Georgi, Phys. Lett. B **513** (2001) 232 [arXiv:hep-ph/0105239].
- [14] J. F. Gunion, H. E. Haber, G. L. Kane and S. Dawson, *The Higgs Hunter's Guide*, Front. Phys. **80** (2000) 1.
- [15] M. Gomez-Bock, M. Mondragon, M. Muhlleitner, M. Spira and P. M. Zerwas, *Concepts of Electroweak Symmetry Breaking and Higgs Physics*, CERN Latin American School on High Energy Physics, Chile 2007, arXiv:0712.2419 [hep-ph].
- [16] A. Djouadi, Phys. Rept. **457** (2008) 1 [arXiv:hep-ph/0503172]; and Phys. Rept. **459** (2008) 1 [arXiv:hep-ph/0503173].
- [17] G. Bernardi, M. Carena and T. Junk *in* K. Nakamura *et al.* [Particle Data Group], J. Phys. G **37** (2010) 075021.
- [18] B. W. Lee, C. Quigg and H. B. Thacker, Phys. Rev. D **16** (1977) 1519.
- [19] N. Cabibbo, L. Maiani, G. Parisi and R. Petronzio, Nucl. Phys. B **158** (1979) 295; M. Sher, Phys. Rept. **179** (1989) 273.
- [20] H. Georgi, H. R. Quinn and S. Weinberg, Phys. Rev. Lett. **33** (1974) 451.
- [21] J. Ellis, J. R. Espinosa, G. F. Giudice, A. Hoecker and A. Riotto, Phys. Lett. B **679** (2009) 369 [arXiv:0906.0954 [hep-ph]].
- [22] G. 't Hooft, Nucl. Phys. B **35** (1971) 167; G. 't Hooft and M. J. G. Veltman, Nucl. Phys. B **44** (1972) 189.
- [23] M. J. G. Veltman, Acta Phys. Polon. B **8** (1977) 475.
- [24] LEP Electroweak Working Group, <http://lepewwg.web.cern.ch/LEPEWWG/>, Oct. 2011.
- [25] J. D. Bjorken, *Weak Interaction Theory and Neutral Currents*, SLAC Summer Institute, Stanford, 1976.
- [26] J. R. Ellis, M. K. Gaillard and D. V. Nanopoulos, Nucl. Phys. B **106** (1976) 292; B. W. Lee, C. Quigg and H. B. Thacker, Phys. Rev. D **16** (1977) 1519; B. L. Ioffe and V. A. Khoze, Sov. J. Part. Nucl. **9** (1978) 50 [Fiz. Elem. Chast. Atom. Yadra **9** (1978) 118].
- [27] D. R. T. Jones and S. T. Petcov, Phys. Lett. B **84** (1979) 440; R. N. Cahn and S. Dawson, Phys. Lett. B **136** (1984) 196 [Erratum-*ibid.* B **138** (1984) 464].
- [28] W. Kilian, M. Kramer and P. M. Zerwas, Phys. Lett. B **373**, 135 (1996) [arXiv:hep-ph/9512355].

[29] H. M. Georgi, S. L. Glashow, M. E. Machacek and D. V. Nanopoulos, Phys. Rev. Lett. **40** (1978) 692.

[30] A. Djouadi, M. Spira and P. M. Zerwas, Phys. Lett. B **264** (1991) 440, and S. Dawson, Nucl. Phys. B **359** (1991) 283; M. Spira, A. Djouadi, D. Graudenz and P. M. Zerwas, Nucl. Phys. B **453** (1995) 17 [arXiv:hep-ph/9504378].

[31] S. Actis, G. Passarino, C. Sturm and S. Uccirati, Phys. Lett. B **670** (2008) 12 [arXiv:0809.1301 [hep-ph]].

[32] R. V. Harlander and W. B. Kilgore, Phys. Rev. Lett. **88** (2002) 201801 [arXiv:hep-ph/0201206]; A. Pak, M. Rogal and M. Steinhauser, JHEP **1002** (2010) 025 [arXiv:0911.4662 [hep-ph]].

[33] S. Moch and A. Vogt, Phys. Lett. B **631** (2005) 48 [arXiv:hep-ph/0508265].

[34] D. L. Rainwater, D. Zeppenfeld and K. Hagiwara, Phys. Rev. D **59** (1998) 014037 [arXiv:hep-ph/9808468]; N. Kauer, T. Plehn, D. L. Rainwater and D. Zeppenfeld, Phys. Lett. B **503** (2001) 113 [arXiv:hep-ph/0012351].

[35] Yu. A. Golfand and E. P. Likhtman, JETP Lett. **13** (1971) 323 [Pisma Zh. Eksp. Teor. Fiz. **13** (1971) 452]; J. Wess and B. Zumino, Nucl. Phys. B **70** (1974) 39.

[36] E. Witten, Phys. Lett. B **105** (1981) 267.

[37] J. F. Gunion and H. E. Haber, Nucl. Phys. B **272** (1986) 1 [Erratum-ibid. B **402** (1993) 567]; Nucl. Phys. B **278** (1986) 449.

[38] G. Degrassi, S. Heinemeyer, W. Hollik, P. Slavich and G. Weiglein, Eur. Phys. J. C **28** (2003) 133 [arXiv:hep-ph/0212020]; M. S. Carena, S. Heinemeyer, C. E. M. Wagner and G. Weiglein, Eur. Phys. J. C **26** (2003) 601 [arXiv:hep-ph/0202167].

[39] J. Bagger *et al.*, Phys. Rev. D **49** (1994) 1246 [arXiv:hep-ph/9306256]; *ibid.* D **52** (1995) 3878 [arXiv:hep-ph/9504426]; E. Boos, H. J. He, W. Kilian, A. Pukhov, C. P. Yuan and P. M. Zerwas, Phys. Rev. D **57** (1998) 1553 [arXiv:hep-ph/9708310]; *ibid.* D **61** (2000) 077901 [arXiv:hep-ph/9908409].

[40] T. Han, H. E. Logan, B. McElrath and L. T. Wang, Phys. Rev. D **67** (2003) 095004 [arXiv:hep-ph/0301040].

[41] N. Arkani-Hamed, M. Porrati and L. Randall, JHEP **0108** (2001) 017 [arXiv:hep-th/0012148].

[42] C. Csaki, C. Grojean, H. Murayama, L. Pilo and J. Terning, Phys. Rev. D **69** (2004) 055006 [arXiv:hep-ph/0305237]; C. Csaki, C. Grojean, L. Pilo and J. Terning, Phys. Rev. Lett. **92** (2004) 101802 [arXiv:hep-ph/0308038].

- [43] ALEPH, DELPHI, L3 and OPAL Collaborations, The LEP Working Group for Higgs Boson Searches, *Searches for Higgs bosons: Preliminary combined results using LEP data collected at energies up to 202 GeV*, CERN-EP/2000-055, unpublished.
- [44] ALEPH, DELPHI, L3 and OPAL Collaborations, The LEP Working Group for Higgs Boson Searches, *Phys. Lett.* **B565** (2003) 61.
- [45] The LEP Working Group for Higgs Boson Searches consists of members of the four LEP Collaborations and a few theorists.
- [46] ALEPH Collaboration, R. Barate *et al.*, *Phys. Lett.* **B526** (2002) 191; DELPHI Collaboration, J. Abdallah *et al.*, *Eur. Phys.J.* **C32** (2004) 145; L3 Collaboration, M. Acciarri *et al.*, *Phys. Lett.* **B517** (2001) 319; OPAL Collaboration, G. Abbiendi *et al.*, *Eur. Phys.J.* **C26** (2003) 479.
- [47] G. Cowan *in* K. Nakamura *et al.*, (Particle Data Group), *J. Phys.* **G37**, 075021 (2010).
- [48] CDF and D0 Collaborations, *Combined CDF and D0 Upper Limits on Standard Model Higgs Boson Production with up to 8.6 fb^{-1} of Data*, [arXiv:hep-ex/1107.5518].
- [49] ATLAS Collaboration, *Limits on the production of the Standard Model Higgs Boson in pp collisions at $\sqrt{s} = 7$ TeV with the ATLAS detector*, accepted by *Eur. Phys. J. C* (2011). [arXiv:hep-ex/1106.2748].
- [50] CMS Collaboration, S. Chatrchyan *et al.*, *Phys. Lett.* **B699** (2011) 25.
- [51] F. Gianotti (ATLAS) and G. Tonelli (CMS), CERN Public Seminar, 13 Dec 2011, [<http://indico.cern.ch/conferenceDisplay.py?confId=164890>].
- [52] ALEPH, DELPHI, L3 and OPAL Collaborations, The LEP Working Group for Higgs Boson Searches, *Eur. Phys. J.* **C47** (2006) 547.
- [53] M. Carena, S. Heinemeyer, C.E.M. Wagner, G. Weiglein, *Eur. Phys. J.* **C26** (2003) 601.
- [54] S. Ambrosanio *et al.*, *Nucl. Phys.* **B624** (2002) 3.